

MIT Open Access Articles

Evidence for the Baryonic Decay $[\bar{B}]^0 \rightarrow D^0 \Lambda^0$

The MIT Faculty has made this article openly available. **Please share** how this access benefits you. Your story matters.

Citation: Lees, J. P., V. Poireau, V. Tisserand, E. Grauges, A. Palano, G. Eigen, B. Stugu, et al. "Evidence for the Baryonic Decay $[\bar{B}]^0 \rightarrow D^0 \Lambda^0$." Phys. Rev. D 89, no. 11 (June 2014). © 2014 American Physical Society

As Published: <http://dx.doi.org/10.1103/PhysRevD.89.112002>

Publisher: American Physical Society

Persistent URL: <http://hdl.handle.net/1721.1/91204>

Version: Final published version: final published article, as it appeared in a journal, conference proceedings, or other formally published context

Terms of Use: Article is made available in accordance with the publisher's policy and may be subject to US copyright law. Please refer to the publisher's site for terms of use.



Evidence for the baryonic decay $\bar{B}^0 \rightarrow D^0 \Lambda \bar{\Lambda}$

J. P. Lees,¹ V. Poireau,¹ V. Tisserand,¹ E. Grauges,² A. Palano,^{3a,3b} G. Eigen,⁴ B. Stugu,⁴ D. N. Brown,⁵ L. T. Kerth,⁵ Yu. G. Kolomensky,⁵ M. J. Lee,⁵ G. Lynch,⁵ H. Koch,⁶ T. Schroeder,⁶ C. Hearty,⁷ T. S. Mattison,⁷ J. A. McKenna,⁷ R. Y. So,⁷ A. Khan,⁸ V. E. Blinov,^{9a,9c} A. R. Buzykaev,^{9a} V. P. Druzhinin,^{9a,9b} V. B. Golubev,^{9a,9b} E. A. Kravchenko,^{9a,9b} A. P. Onuchin,^{9a,9c} S. I. Serednyakov,^{9a,9b} Yu. I. Skovpen,^{9a,9b} E. P. Solodov,^{9a,9b} K. Yu. Todyshev,^{9a,9b} A. N. Yushkov,^{9a} D. Kirkby,¹⁰ A. J. Lankford,¹⁰ M. Mandelkern,¹⁰ B. Dey,¹¹ J. W. Gary,¹¹ O. Long,¹¹ G. M. Vitug,¹¹ C. Campagnari,¹² M. Franco Sevilla,¹² T. M. Hong,¹² D. Kovalskyi,¹² J. D. Richman,¹² C. A. West,¹² A. M. Eisner,¹³ W. S. Lockman,¹³ B. A. Schumm,¹³ A. Seiden,¹³ D. S. Chao,¹⁴ C. H. Cheng,¹⁴ B. Echenard,¹⁴ K. T. Flood,¹⁴ D. G. Hitlin,¹⁴ P. Ongmongkolkul,¹⁴ F. C. Porter,¹⁴ R. Andreassen,¹⁵ Z. Huard,¹⁵ B. T. Meadows,¹⁵ B. G. Pushpawela,¹⁵ M. D. Sokoloff,¹⁵ L. Sun,¹⁵ P. C. Bloom,¹⁶ W. T. Ford,¹⁶ A. Gaz,¹⁶ U. Nauenberg,¹⁶ J. G. Smith,¹⁶ S. R. Wagner,¹⁶ R. Ayad,^{17,†} W. H. Toki,¹⁷ B. Spaan,¹⁸ R. Schwierz,¹⁹ D. Bernard,²⁰ M. Verderi,²⁰ S. Playfer,²¹ D. Bettoni,^{22a} C. Bozzi,^{22a} R. Calabrese,^{22a,22b} G. Cibinetto,^{22a,22b} E. Fioravanti,^{22a,22b} I. Garzia,^{22a,22b} E. Luppi,^{22a,22b} L. Piemontese,^{22a} V. Santoro,^{22a} R. Baldini-Ferroli,²³ A. Calcaterra,²³ R. de Sangro,²³ G. Finocchiaro,²³ S. Martellotti,²³ P. Patteri,²³ I. M. Peruzzi,^{23,‡} M. Piccolo,²³ M. Rama,²³ A. Zallo,²³ R. Contri,^{24a,24b} E. Guido,^{24a,24b} M. Lo Vetere,^{24a,24b} M. R. Monge,^{24a,24b} S. Passaggio,^{24a} C. Patrignani,^{24a,24b} E. Robutti,^{24a} B. Bhuyan,²⁵ V. Prasad,²⁵ M. Morii,²⁶ A. Adametz,²⁷ U. Uwer,²⁷ H. M. Lacker,²⁸ P. D. Dauncey,²⁹ U. Mallik,³⁰ C. Chen,³¹ J. Cochran,³¹ W. T. Meyer,³¹ S. Prell,³¹ A. V. Gritsan,³² N. Arnaud,³³ M. Davier,³³ D. Derkach,³³ G. Grosdidier,³³ F. Le Diberder,³³ A. M. Lutz,³³ B. Malaescu,^{33,§} P. Roudeau,³³ A. Stocchi,³³ G. Wormser,³³ D. J. Lange,³⁴ D. M. Wright,³⁴ J. P. Coleman,³⁵ J. R. Fry,³⁵ E. Gabathuler,³⁵ D. E. Hutchcroft,³⁵ D. J. Payne,³⁵ C. Touramanis,³⁵ A. J. Bevan,³⁶ F. Di Lodovico,³⁶ R. Sacco,³⁶ G. Cowan,³⁷ J. Bougher,³⁸ D. N. Brown,³⁸ C. L. Davis,³⁸ A. G. Denig,³⁹ M. Fritsch,³⁹ W. Gradl,³⁹ K. Griessinger,³⁹ A. Hafner,³⁹ E. Prencipe,³⁹ K. R. Schubert,³⁹ R. J. Barlow,^{40,||} G. D. Lafferty,⁴⁰ E. Behn,⁴¹ R. Cenci,⁴¹ B. Hamilton,⁴¹ A. Jawahery,⁴¹ D. A. Roberts,⁴¹ R. Cowan,⁴² D. Dujmic,⁴² G. Sciolla,⁴² R. Cheaib,⁴³ P. M. Patel,^{43,*} S. H. Robertson,⁴³ P. Biassoni,^{44a,44b} N. Neri,^{44a} F. Palombo,^{44a,44b} L. Cremaldi,⁴⁵ R. Godang,^{45,¶} P. Sonnek,⁴⁵ D. J. Summers,⁴⁵ M. Simard,⁴⁶ P. Taras,⁴⁶ G. De Nardo,^{47a,47b} D. Monorchio,^{47a,47b} G. Onorato,^{47a,47b} C. Sciacca,^{47a,47b} M. Martinelli,⁴⁸ G. Raven,⁴⁸ C. P. Jessop,⁴⁹ J. M. LoSecco,⁴⁹ K. Honscheid,⁵⁰ R. Kass,⁵⁰ J. Brau,⁵¹ R. Frey,⁵¹ N. B. Sinev,⁵¹ D. Strom,⁵¹ E. Torrence,⁵¹ E. Feltresi,^{52a,52b} M. Margoni,^{52a,52b} M. Morandin,^{52a} M. Posocco,^{52a} M. Rotondo,^{52a} G. Simi,^{52a} F. Simonetto,^{52a,52b} R. Stroili,^{52a,52b} S. Akar,⁵³ E. Ben-Haim,⁵³ M. Bomben,⁵³ G. R. Bonneaud,⁵³ H. Briand,⁵³ G. Calderini,⁵³ J. Chauveau,⁵³ Ph. Leruste,⁵³ G. Marchiori,⁵³ J. Ocariz,⁵³ S. Sitt,⁵³ M. Biasini,^{54a,54b} E. Manoni,^{54a} S. Pacetti,^{54a,54b} A. Rossi,^{54a} C. Angelini,^{55a,55b} G. Batignani,^{55a,55b} S. Bettarini,^{55a,55b} M. Carpinelli,^{55a,55b,**} G. Casarosa,^{55a,55b} A. Cervelli,^{55a,55b} F. Forti,^{55a,55b} M. A. Giorgi,^{55a,55b} A. Lusiani,^{55a,55c} B. Oberhof,^{55a,55b} E. Paoloni,^{55a,55b} A. Perez,^{55a} G. Rizzo,^{55a,55b} J. J. Walsh,^{55a} D. Lopes Pegna,⁵⁶ J. Olsen,⁵⁶ A. J. S. Smith,⁵⁶ R. Faccini,^{57a,57b} F. Ferrarotto,^{57a} F. Ferroni,^{57a,57b} M. Gaspero,^{57a,57b} L. Li Gioi,^{57a} G. Piredda,^{57a} C. Bünger,⁵⁸ O. Grünberg,⁵⁸ T. Hartmann,⁵⁸ T. Leddig,⁵⁸ C. Voß,⁵⁸ R. Waldi,⁵⁸ T. Adye,⁵⁹ E. O. Olaiya,⁵⁹ F. F. Wilson,⁵⁹ S. Emery,⁶⁰ G. Hamel de Monchenault,⁶⁰ G. Vasseur,⁶⁰ Ch. Yèche,⁶⁰ F. Anulli,^{61,††} D. Aston,⁶¹ D. J. Bard,⁶¹ J. F. Benitez,⁶¹ C. Cartaro,⁶¹ M. R. Convery,⁶¹ J. Dorfan,⁶¹ G. P. Dubois-Felsmann,⁶¹ W. Dunwoodie,⁶¹ M. Ebert,⁶¹ R. C. Field,⁶¹ B. G. Fulsom,⁶¹ A. M. Gabareen,⁶¹ M. T. Graham,⁶¹ C. Hast,⁶¹ W. R. Innes,⁶¹ P. Kim,⁶¹ M. L. Kocian,⁶¹ D. W. G. S. Leith,⁶¹ P. Lewis,⁶¹ D. Lindemann,⁶¹ B. Lindquist,⁶¹ S. Luitz,⁶¹ V. Luth,⁶¹ H. L. Lynch,⁶¹ D. B. MacFarlane,⁶¹ D. R. Muller,⁶¹ H. Neal,⁶¹ S. Nelson,⁶¹ M. Perl,⁶¹ T. Pulliam,⁶¹ B. N. Ratcliff,⁶¹ A. Roodman,⁶¹ A. A. Salnikov,⁶¹ R. H. Schindler,⁶¹ A. Snyder,⁶¹ D. Su,⁶¹ M. K. Sullivan,⁶¹ J. Va'vra,⁶¹ A. P. Wagner,⁶¹ W. F. Wang,⁶¹ W. J. Wisniewski,⁶¹ M. Wittgen,⁶¹ D. H. Wright,⁶¹ H. W. Wulsin,⁶¹ V. Ziegler,⁶¹ W. Park,⁶² M. V. Purohit,⁶² R. M. White,^{62,‡‡} J. R. Wilson,⁶² A. Randle-Conde,⁶³ S. J. Sekula,⁶³ M. Bellis,⁶⁴ P. R. Burchat,⁶⁴ T. S. Miyashita,⁶⁴ E. M. T. Puccio,⁶⁴ M. S. Alam,⁶⁵ J. A. Ernst,⁶⁵ R. Gorodeisky,⁶⁶ N. Guttman,⁶⁶ D. R. Peimer,⁶⁶ A. Soffer,⁶⁶ S. M. Spanier,⁶⁷ J. L. Ritchie,⁶⁸ A. M. Ruland,⁶⁸ R. F. Schwitters,⁶⁸ B. C. Wray,⁶⁸ J. M. Izen,⁶⁹ X. C. Lou,⁶⁹ F. Bianchi,^{70a,70b} F. De Mori,^{70a,70b} A. Filippi,^{70a} D. Gamba,^{70a,70b} S. Zambito,^{70a,70b} L. Lanceri,^{71a,71b} L. Vitale,^{71a,71b} F. Martinez-Vidal,⁷² A. Oyanguren,⁷² P. Villanueva-Perez,⁷² H. Ahmed,⁷³ J. Albert,⁷³ Sw. Banerjee,⁷³ F. U. Bernlochner,⁷³ H. H. F. Choi,⁷³ G. J. King,⁷³ R. Kowalewski,⁷³ M. J. Lewczuk,⁷³ T. Lueck,⁷³ I. M. Nugent,⁷³ J. M. Roney,⁷³ R. J. Sobie,⁷³ N. Tasneem,⁷³ T. J. Gershon,⁷⁴ P. F. Harrison,⁷⁴ T. E. Latham,⁷⁴ H. R. Band,⁷⁵ S. Dasu,⁷⁵ Y. Pan,⁷⁵ R. Prepost,⁷⁵ and S. L. Wu⁷⁵

(BABAR Collaboration)

¹Laboratoire d'Annecy-le-Vieux de Physique des Particules (LAPP), Université de Savoie, CNRS/IN2P3, F-74941 Annecy-Le-Vieux, France

²Universitat de Barcelona, Facultat de Física, Departament ECM, E-08028 Barcelona, Spain

^{3a}INFN Sezione di Bari, I-70126 Bari, Italy

^{3b}Dipartimento di Fisica, Università di Bari, I-70126 Bari, Italy

⁴University of Bergen, Institute of Physics, N-5007 Bergen, Norway

⁵Lawrence Berkeley National Laboratory and University of California, Berkeley, California 94720, USA

- ⁶Ruhr Universität Bochum, Institut für Experimentalphysik 1, D-44780 Bochum, Germany
- ⁷University of British Columbia, Vancouver, British Columbia, Canada V6T 1Z1
- ⁸Brunel University, Uxbridge, Middlesex UB8 3PH, United Kingdom
- ^{9a}Budker Institute of Nuclear Physics SB RAS, Novosibirsk 630090, Russia
- ^{9b}Novosibirsk State University, Novosibirsk 630090, Russia
- ^{9c}Novosibirsk State Technical University, Novosibirsk 630092, Russia
- ¹⁰University of California at Irvine, Irvine, California 92697, USA
- ¹¹University of California at Riverside, Riverside, California 92521, USA
- ¹²University of California at Santa Barbara, Santa Barbara, California 93106, USA
- ¹³University of California at Santa Cruz, Institute for Particle Physics, Santa Cruz, California 95064, USA
- ¹⁴California Institute of Technology, Pasadena, California 91125, USA
- ¹⁵University of Cincinnati, Cincinnati, Ohio 45221, USA
- ¹⁶University of Colorado, Boulder, Colorado 80309, USA
- ¹⁷Colorado State University, Fort Collins, Colorado 80523, USA
- ¹⁸Technische Universität Dortmund, Fakultät Physik, D-44221 Dortmund, Germany
- ¹⁹Technische Universität Dresden, Institut für Kern- und Teilchenphysik, D-01062 Dresden, Germany
- ²⁰Laboratoire Leprince-Ringuet, Ecole Polytechnique, CNRS/IN2P3, F-91128 Palaiseau, France
- ²¹University of Edinburgh, Edinburgh EH9 3JZ, United Kingdom
- ^{22a}INFN Sezione di Ferrara, I-44122 Ferrara, Italy
- ^{22b}Dipartimento di Fisica e Scienze della Terra, Università di Ferrara, I-44122 Ferrara, Italy
- ²³INFN Laboratori Nazionali di Frascati, I-00044 Frascati, Italy
- ^{24a}INFN Sezione di Genova, I-16146 Genova, Italy
- ^{24b}Dipartimento di Fisica, Università di Genova, I-16146 Genova, Italy
- ²⁵Indian Institute of Technology Guwahati, Guwahati, Assam 781 039, India
- ²⁶Harvard University, Cambridge, Massachusetts 02138, USA
- ²⁷Universität Heidelberg, Physikalisches Institut, D-69120 Heidelberg, Germany
- ²⁸Humboldt-Universität zu Berlin, Institut für Physik, D-12489 Berlin, Germany
- ²⁹Imperial College London, London SW7 2AZ, United Kingdom
- ³⁰University of Iowa, Iowa City, Iowa 52242, USA
- ³¹Iowa State University, Ames, Iowa 50011-3160, USA
- ³²Johns Hopkins University, Baltimore, Maryland 21218, USA
- ³³Laboratoire de l'Accélérateur Linéaire, IN2P3/CNRS et Université Paris-Sud 11, Centre Scientifique d'Orsay, F-91898 Orsay Cedex, France
- ³⁴Lawrence Livermore National Laboratory, Livermore, California 94550, USA
- ³⁵University of Liverpool, Liverpool L69 7ZE, United Kingdom
- ³⁶Queen Mary, University of London, London E1 4NS, United Kingdom
- ³⁷University of London, Royal Holloway and Bedford New College, Egham, Surrey TW20 0EX, United Kingdom
- ³⁸University of Louisville, Louisville, Kentucky 40292, USA
- ³⁹Johannes Gutenberg-Universität Mainz, Institut für Kernphysik, D-55099 Mainz, Germany
- ⁴⁰University of Manchester, Manchester M13 9PL, United Kingdom
- ⁴¹University of Maryland, College Park, Maryland 20742, USA
- ⁴²Massachusetts Institute of Technology, Laboratory for Nuclear Science, Cambridge, Massachusetts 02139, USA
- ⁴³McGill University, Montréal, Québec, Canada H3A 2T8
- ^{44a}INFN Sezione di Milano, I-20133 Milano, Italy
- ^{44b}Dipartimento di Fisica, Università di Milano, I-20133 Milano, Italy
- ⁴⁵University of Mississippi, University, Mississippi 38677, USA
- ⁴⁶Université de Montréal, Physique des Particules, Montréal, Québec, Canada H3C 3J7
- ^{47a}INFN Sezione di Napoli, I-80126 Napoli, Italy
- ^{47b}Dipartimento di Scienze Fisiche, Università di Napoli Federico II, I-80126 Napoli, Italy
- ⁴⁸NIKHEF, National Institute for Nuclear Physics and High Energy Physics, NL-1009 DB Amsterdam, The Netherlands
- ⁴⁹University of Notre Dame, Notre Dame, Indiana 46556, USA
- ⁵⁰Ohio State University, Columbus, Ohio 43210, USA
- ⁵¹University of Oregon, Eugene, Oregon 97403, USA
- ^{52a}INFN Sezione di Padova, I-35131 Padova, Italy
- ^{52b}Dipartimento di Fisica, Università di Padova, I-35131 Padova, Italy
- ⁵³Laboratoire de Physique Nucléaire et de Hautes Energies, IN2P3/CNRS, Université Pierre et Marie Curie-Paris6, Université Denis Diderot-Paris7, F-75252 Paris, France

- ^{54a}INFN Sezione di Perugia, I-06123 Perugia, Italy
^{54b}Dipartimento di Fisica, Università di Perugia, I-06123 Perugia, Italy
^{55a}INFN Sezione di Pisa, I-56127 Pisa, Italy
^{55b}Dipartimento di Fisica, Università di Pisa, I-56127 Pisa, Italy
^{55c}Scuola Normale Superiore di Pisa, I-56127 Pisa, Italy
⁵⁶Princeton University, Princeton, New Jersey 08544, USA
^{57a}INFN Sezione di Roma, I-00185 Roma, Italy
^{57b}Dipartimento di Fisica, Università di Roma La Sapienza, I-00185 Roma, Italy
⁵⁸Universität Rostock, D-18051 Rostock, Germany
⁵⁹Rutherford Appleton Laboratory, Chilton, Didcot, Oxon, OX11 0QX, United Kingdom
⁶⁰CEA, Irfu, SPP, Centre de Saclay, F-91191 Gif-sur-Yvette, France
⁶¹SLAC National Accelerator Laboratory, Stanford, California 94309 USA
⁶²University of South Carolina, Columbia, South Carolina 29208, USA
⁶³Southern Methodist University, Dallas, Texas 75275, USA
⁶⁴Stanford University, Stanford, California 94305-4060, USA
⁶⁵State University of New York, Albany, New York 12222, USA
⁶⁶Tel Aviv University, School of Physics and Astronomy, Tel Aviv 69978, Israel
⁶⁷University of Tennessee, Knoxville, Tennessee 37996, USA
⁶⁸University of Texas at Austin, Austin, Texas 78712, USA
⁶⁹University of Texas at Dallas, Richardson, Texas 75083, USA
^{70a}INFN Sezione di Torino, I-10125 Torino, Italy
^{70b}Dipartimento di Fisica, Università di Torino, I-10125 Torino, Italy
^{71a}INFN Sezione di Trieste, I-34127 Trieste, Italy
^{71b}Dipartimento di Fisica, Università di Trieste, I-34127 Trieste, Italy
⁷²IFIC, Universitat de Valencia-CSIC, E-46071 Valencia, Spain
⁷³University of Victoria, Victoria, British Columbia, Canada V8W 3P6
⁷⁴Department of Physics, University of Warwick, Coventry CV4 7AL, United Kingdom
⁷⁵University of Wisconsin, Madison, Wisconsin 53706, USA
(Received 27 January 2014; published 6 June 2014)

Evidence is presented for the baryonic B meson decay $\bar{B}^0 \rightarrow D^0 \Lambda \bar{\Lambda}$ based on a data sample of 471×10^6 $B\bar{B}$ pairs collected with the BABAR detector at the PEP-II asymmetric e^+e^- collider located at the SLAC National Accelerator Laboratory. The branching fraction is determined to be $\mathcal{B}(\bar{B}^0 \rightarrow D^0 \Lambda \bar{\Lambda}) = (9.8_{-2.6}^{+2.9} \pm 1.9) \times 10^{-6}$, corresponding to a significance of 3.4 standard deviations including additive systematic uncertainties. A search for the related baryonic B meson decay $\bar{B}^0 \rightarrow D^0 \Sigma^0 \bar{\Lambda}$ with $\Sigma^0 \rightarrow \Lambda \gamma$ is performed and an upper limit $\mathcal{B}(\bar{B}^0 \rightarrow D^0 \Sigma^0 \bar{\Lambda} + \bar{B}^0 \rightarrow D^0 \Lambda \bar{\Sigma}^0) < 3.1 \times 10^{-5}$ is determined at 90% confidence level.

DOI: 10.1103/PhysRevD.89.112002

PACS numbers: 13.25.Hw, 13.60.Rj, 14.20.Lq

I. INTRODUCTION

Little is known about the mechanism of baryon production in weak decays or in the hadronization process. Baryons

are produced in $(6.8 \pm 0.6)\%$ of all B meson decays [1]. Due to this large rate, B meson decays can provide important information about baryon production. Due to the low energy scale, perturbative quantum chromodynamics (QCD) cannot be applied to this process. Furthermore, lattice QCD calculations are not available. The description of baryonic B decays thus relies on phenomenological models.

Pole models [2] are a common tool used in theoretical studies of hadronic decays. Meson pole models predict an enhancement at low baryon-antibaryon masses. In many three-body decays into a baryon, an antibaryon and a meson, the baryon-antibaryon pair, can be described by a meson pole, i.e., the decay of a virtual meson with a mass below threshold. This leads to a steeply falling amplitude at the threshold of the baryon-antibaryon mass and explains the enhancement observed in decays such as $B^- \rightarrow \Lambda_c \bar{p} \pi^-$ [3,4], $B^- \rightarrow p \bar{p} K^-$ [5–7], and $\bar{B}^0 \rightarrow D^0 p \bar{p}$ [8,9].

*Deceased.

[†]Present address: The University of Tabuk, Tabuk 71491, Saudi Arabia.

[‡]Also at Università di Perugia, Dipartimento di Fisica, Perugia, Italy.

[§]Present address: Laboratoire de Physique Nucléaire et de Hautes Energies, IN2P3/CNRS, Paris, France.

^{||}Present address: The University of Huddersfield, Huddersfield HD1 3DH, United Kingdom.

[¶]Present address: University of South Alabama, Mobile, Alabama 36688, USA.

^{**}Also at Università di Sassari, Sassari, Italy.

^{††}Also at INFN Sezione di Roma, Roma, Italy.

^{‡‡}Present address: Universidad Técnica Federico Santa María, Valparaíso, Chile 2390123.

In addition to the meson pole models described above, there are baryon pole models in which the initial state decays through the strong interaction into a pair of baryons. Then, one of these baryons decays via the weak interaction into a baryon and a meson. For such baryon pole models, no enhancement at threshold in the dibaryon invariant mass is expected.

The decay of a B meson into a D^0 meson and a pair of baryons has been the subject of several theoretical investigations [10,11]. Reference [11] predicts the branching fractions for $\bar{B}^0 \rightarrow D^0 \Lambda \bar{\Lambda}$ decays and for the sum of the $\bar{B}^0 \rightarrow D^0 \Lambda \bar{\Sigma}^0$ and $\bar{B}^0 \rightarrow D^0 \Sigma^0 \bar{\Lambda}$ decays to be

$$\begin{aligned} \mathcal{B}(\bar{B}^0 \rightarrow D^0 \Lambda \bar{\Lambda}) &= (2 \pm 1) \times 10^{-6}, \\ \mathcal{B}(\bar{B}^0 \rightarrow D^0 \Lambda \bar{\Sigma}^0 + \bar{B}^0 \rightarrow D^0 \Sigma^0 \bar{\Lambda}) &= (1.8 \pm 0.5) \times 10^{-5}. \end{aligned} \quad (1)$$

It is impractical to separate the $\bar{B}^0 \rightarrow D^0 \Lambda \bar{\Sigma}^0$ and $\bar{B}^0 \rightarrow D^0 \Sigma^0 \bar{\Lambda}$ decays since each leads to the final state $\Lambda \bar{\Lambda} \gamma$.

As can be seen from the Feynman diagrams shown in Fig. 1, the only difference between the $\bar{B}^0 \rightarrow D^0 p \bar{p}$ decay on the one hand and the $\bar{B}^0 \rightarrow D^0 \Lambda \bar{\Lambda}$ and $\bar{B}^0 \rightarrow D^0 \Sigma^0 \bar{\Lambda}$ decays on the other hand is the replacement of a $u\bar{u}$ pair with an $s\bar{s}$ pair. In the hadronization process, $s\bar{s}$ -pair production is suppressed by about a factor of three compared to $u\bar{u}$ - or $d\bar{d}$ -pair production [12]. Furthermore, since both Λ and Σ^0 baryons can be produced, there are four possible final states with an $s\bar{s}$ pair ($\Lambda \bar{\Lambda}$, $\Lambda \bar{\Sigma}^0$, $\Sigma^0 \bar{\Lambda}$, and $\Sigma^0 \bar{\Sigma}^0$) compared to only one for a $u\bar{u}$ pair ($p \bar{p}$), neglecting the production of excited baryons. Assuming equal production rates for these four modes and that the spin-1/2 states dominate, a suppression of a factor of ~ 12 is expected for $\bar{B}^0 \rightarrow D^0 \Lambda \bar{\Lambda}$ decays compared to $\bar{B}^0 \rightarrow D^0 p \bar{p}$ decays, where the branching fraction of the latter process is $\mathcal{B}(\bar{B}^0 \rightarrow D^0 p \bar{p}) = (1.04 \pm 0.04) \times 10^{-4}$ [1].

The branching fraction for $\bar{B}^0 \rightarrow D^0 \Lambda \bar{\Lambda}$ has been measured by the Belle Collaboration to be $\mathcal{B}(\bar{B}^0 \rightarrow D^0 \Lambda \bar{\Lambda}) = (10.5^{+5.7}_{-4.4} \pm 1.4) \times 10^{-6}$ [13]. There are no previous results for the $\bar{B}^0 \rightarrow D^0 \Sigma^0 \bar{\Lambda}$ decay mode.

II. THE BABAR EXPERIMENT

This analysis is based on a data sample of 429 fb^{-1} [14], corresponding to 471×10^6 $B\bar{B}$ pairs, collected with the *BABAR* detector at the PEP-II asymmetric-energy e^+e^- collider at the SLAC National Accelerator Laboratory at center-of-mass energies near and equal to the $\Upsilon(4S)$ mass. The reconstruction efficiency is determined through use of Monte Carlo (MC) simulation, based on the EVTGEN [15] program for the event generation and the GEANT4 [16] package for modeling of the detector response. The MC events are generated uniformly in the $\bar{B}^0 \rightarrow D^0 \Lambda \bar{\Lambda}$ and $\bar{B}^0 \rightarrow D^0 \Sigma^0 \bar{\Lambda}$ phase space.

The *BABAR* detector is described in detail elsewhere [17,18]. Charged particle trajectories are measured with a five-layer double-sided silicon vertex tracker and a 40-layer drift chamber immersed in a 1.5 T axial magnetic field. Charged particle identification is provided by ionization energy measurements in the tracking chambers and by Cherenkov-radiation photons recorded with an internally reflecting ring-imaging detector. Electrons and photons are reconstructed with an electromagnetic calorimeter.

III. RECONSTRUCTION OF Λ BARYON, D^0 MESON, AND \bar{B}^0 MESON CANDIDATES

We reconstruct Λ baryons through the decay mode $\Lambda \rightarrow p\pi^-$ and D^0 mesons through the modes $D^0 \rightarrow K^-\pi^+$, $D^0 \rightarrow K^-\pi^+\pi^+\pi^-$, and $D^0 \rightarrow K^-\pi^+\pi^0$ [19]. Charged kaon and proton candidates are required to satisfy particle identification criteria. Charged pions are selected as charged tracks that are not identified as a kaon or proton.

Candidate π^0 mesons are reconstructed from two separated energy deposits in the electromagnetic calorimeter not associated with charged tracks. To discriminate against neutral hadrons, the shower shape of each deposit is required to be consistent with that of a photon [20]. Furthermore, we require $E(\gamma_1) > 0.125 \text{ GeV}$ and $E(\gamma_2) > 0.04 \text{ GeV}$, where $E(\gamma_1)$ and $E(\gamma_2)$ are the energies of the photon candidates, with $E(\gamma_1) > E(\gamma_2)$. The photon-photon invariant mass is required to lie in the range $m(\gamma\gamma) \in [0.116, 0.145] \text{ GeV}/c^2$.

The Λ daughters are fit to a common vertex and the reconstructed mass is required to lie within three standard

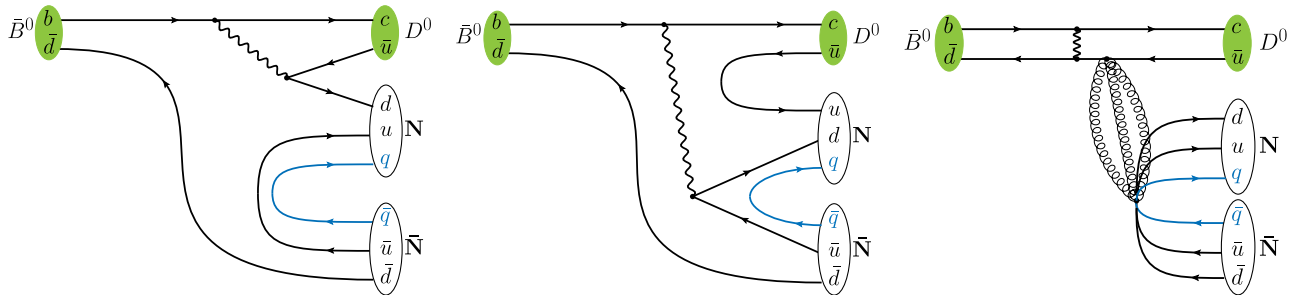


FIG. 1 (color online). Leading-order Feynman diagrams for the decays $\bar{B}^0 \rightarrow D^0 N \bar{N}$. Setting $q = u$ leads to the $D^0 p \bar{p}$ final state and setting $q = s$ to the $D^0 \Lambda \bar{\Lambda}$, $D^0 \Sigma^0 \bar{\Lambda}$, $D^0 \Lambda \bar{\Sigma}^0$, and $D^0 \Sigma^0 \bar{\Sigma}^0$ final states.

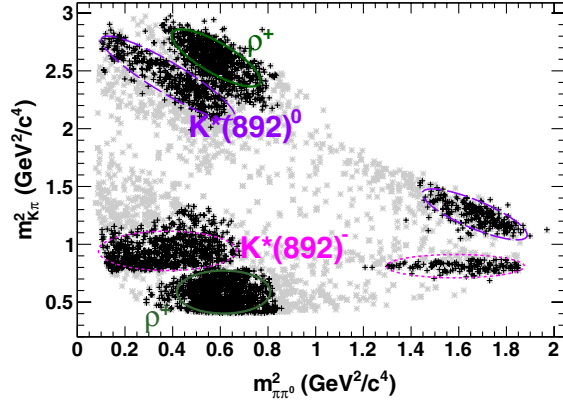


FIG. 2 (color online). Dalitz plot for simulated $D^0 \rightarrow K^-\pi^+\pi^0$ events before (gray stars) and after (black crosses) the $w_{\text{Dalitz}} > 0.02$ requirement. Resonant decays are indicated.

deviations of the nominal value [1], where the standard deviation is the mass resolution. We select Λ candidates by requiring the flight significance L_t/σ_{L_t} to exceed 4, where L_t is the Λ flight length in the transverse plane and σ_{L_t} its uncertainty. The Σ^0 baryons are produced in the decay $\Sigma^0 \rightarrow \Lambda\gamma$, and the photon is not reconstructed.

The D^0 daughter candidates are fit to a common vertex, and the reconstructed mass is required to lie within three times the mass resolution from their nominal values [1]. The signal-to-background ratio for $D^0 \rightarrow K^-\pi^+\pi^0$ is improved by making use of the resonant substructure of this decay, which is well known. Using results from the E691 Collaboration [21], we calculate the probability w_{Dalitz} for a D^0 candidate to be located at a certain position in the Dalitz plane. We require $w_{\text{Dalitz}} > 0.02$. Figure 2 shows the Dalitz plot distributions, based on simulation, for candidates selected with and without the w_{Dalitz} requirement.

The D^0 and Λ candidates are constrained to their nominal masses in the reconstruction of the \bar{B}^0 candidates. We apply a fit to the entire decay chain and require the probability for the vertex fit to be larger than 0.001.

TABLE I. Summary of selection criteria.

Selection criterion	Selected candidates
$\Lambda/\bar{\Lambda}$ mass	$m_{p\pi} \in [1.112, 1.120] \text{ GeV}/c^2$
Flight significance	$L_t/\sigma_{L_t} > 4$
$D^0 \rightarrow K^-\pi$ mass	$m_{K\pi} \in [1.846, 1.882] \text{ GeV}/c^2$
$D^0 \rightarrow K^-\pi^+\pi^-\pi^0$ mass	$m_{K\pi\pi\pi} \in [1.852, 1.876] \text{ GeV}/c^2$
Lateral parameter γ_1	$0.05 < \text{LAT}(\gamma_1) < 0.55$
Lateral parameter γ_2	$\text{LAT}(\gamma_2) > 0.075$
Calorimeter energy γ_1	$E(\gamma_1) > 0.125 \text{ GeV}$
Calorimeter energy γ_2	$E(\gamma_2) > 0.04 \text{ GeV}$
π^0 mass	$m_{\gamma\gamma} \in [0.116, 0.145] \text{ GeV}/c^2$
$D^0 \rightarrow K^-\pi^+\pi^0$ mass	$m_{K\pi\pi^0} \in [1.81, 1.89] \text{ GeV}/c^2$
Dalitz weight	$w_{\text{Dalitz}} > 0.02$
B vertex probability	$p(B) > 0.001$
Fisher discriminant	$\mathcal{F} > 0.1$

To reduce background from $e^+e^- \rightarrow q\bar{q}$ events with $q = u, d, s, c$, we apply a selection on a Fisher discriminant \mathcal{F} that combines the values of $|\cos \theta_{\text{Thr}}|$, where θ_{Thr} is the angle between the thrust axis of the B candidate and the thrust axis formed from the remaining tracks and clusters in the event; $|\cos \theta_z|$, where θ_z is the angle between the B thrust axis and the beam axis; $|\cos \phi|$, where ϕ is the angle between the B momentum and the beam axis; and the normalized second Fox Wolfram moment [22]. All these quantities are defined in the center-of-mass frame. All selection criteria are summarized in Table I.

IV. FIT STRATEGY

We determine the number of signal candidates with a two-dimensional unbinned extended maximum likelihood fit to the invariant mass $m(D^0\Lambda\bar{\Lambda})$ and the energy substituted mass m_{ES} . The latter is defined as

$$m_{\text{ES}} = \sqrt{(s/2 + \mathbf{p}_0 \cdot \mathbf{p}_B)^2/E_0^2 - |\mathbf{p}_B|^2}, \quad (2)$$

where \sqrt{s} is the center-of-mass energy, \mathbf{p}_B the B candidate's momentum, and (E_0, \mathbf{p}_0) the four-momentum vector of the e^+e^- system, each given in the laboratory frame. Both $m(D^0\Lambda\bar{\Lambda})$ and m_{ES} are centered at the B mass for well-reconstructed B decays.

Due to the small mass difference of $76.9 \text{ MeV}/c^2$ [1] between the Λ and Σ^0 baryons, $\bar{B}^0 \rightarrow D^0\Sigma^0\bar{\Lambda}$ decays, where the Σ^0 decays radiatively as $\Sigma^0 \rightarrow \Lambda\gamma$, are a source of background. Such events peak at the B mass in m_{ES} and are slightly shifted in $m(D^0\Lambda\bar{\Lambda})$ with respect to $\bar{B}^0 \rightarrow D^0\Lambda\bar{\Lambda}$ (Fig. 3). We account for this decay by including an explicit term in the likelihood function (see below), whose yield is determined in the fit.

We divide the data sample into three subsamples corresponding to the D^0 decay modes. Given their different signal-to-background ratios, we determine the number of signal candidates in a simultaneous fit to the three independent subsamples. We study simulated samples of signal and background events and find no significant correlation between m_{ES} and $m(D^0\Lambda\bar{\Lambda})$. Therefore, we describe each $\bar{B}^0 \rightarrow D^0\Lambda\bar{\Lambda}$ signal sample with the product of a Novosibirsk function in m_{ES} and a sum of two Gaussian functions f^{GG} in $m(D^0\Lambda\bar{\Lambda})$. The Novosibirsk function is defined as

$$f^{\text{Novo}}(m_{\text{ES}}) = \exp \left[-\frac{1}{2} \left(\frac{\ln^2[1 + \lambda\alpha(m_{\text{ES}} - \mu)]}{\alpha^2} + \alpha^2 \right) \right], \quad (3)$$

$$\lambda = \sinh(\alpha\sqrt{\ln 4})/(\sigma\alpha\sqrt{\ln 4}),$$

with μ the mean value, σ the width, and α the tail parameter. The decay $\bar{B}^0 \rightarrow D^0\Sigma^0\bar{\Lambda}$ is described by the product of a Novosibirsk $f^{\text{Novo1},\Sigma^0}$ function in m_{ES} and a sum of another Novosibirsk function $f^{\text{Novo2},\Sigma^0}$ and a Gaussian \mathcal{G}^{Σ^0} in

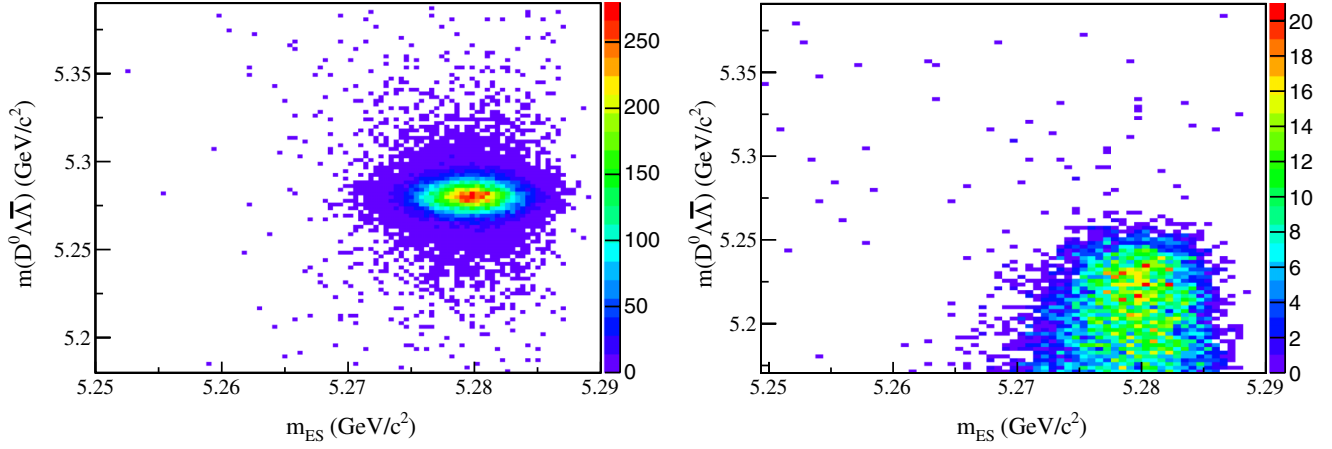


FIG. 3 (color online). Distributions for $\bar{B}^0 \rightarrow D^0 \Lambda \bar{\Lambda}$ (left) and $\bar{B}^0 \rightarrow D^0 \Sigma^0 \bar{\Lambda}$ reconstructed as $\bar{B}^0 \rightarrow D^0 \Lambda \bar{\Lambda}$ (right) for the $D^0 \rightarrow K^- \pi^+$ mode in simulated events.

$m(D^0 \Lambda \bar{\Lambda})$. All parameters are determined using Monte Carlo simulated events and are fixed in the final fit. Background from $e^+ e^- \rightarrow q \bar{q}$ events and other B meson decays is modeled by the product of an ARGUS function [23] in m_{ES} and a first order polynomial in $m(D^0 \Lambda \bar{\Lambda})$.

The full fit function is defined as

$$\begin{aligned}
 f_j^{\text{Fit}} &= f_j^\Lambda + f_j^{\Sigma^0} + f_j^{\text{Bkg}} \\
 &= f_j^{\text{Novo}, \Lambda}(m_{ES}) \times f_j^{GG}(m(D^0 \Lambda \bar{\Lambda})) + f_j^{\text{Novo}, \Sigma^0}(m_{ES}) \\
 &\quad \times [f_j^{\text{Novo}, \Sigma^0}(m(D^0 \Lambda \bar{\Lambda})) + \mathcal{G}_j^{\Sigma^0}(m(D^0 \Lambda \bar{\Lambda}))] \\
 &\quad + f_j^{\text{ARGUS}}(m_{ES}) \times f_j^{\text{Poly}}(m(D^0 \Lambda \bar{\Lambda})), \quad (4)
 \end{aligned}$$

where the index j corresponds to the three D^0 decay modes.

The branching fraction is determined from

$$\begin{aligned}
 \mathcal{B}(\bar{B}^0 \rightarrow D^0 \Lambda \bar{\Lambda}) &= \frac{N(\bar{B}^0 \rightarrow D^0 \Lambda \bar{\Lambda})}{2N_{B^0 \bar{B}^0} \times \bar{\epsilon}} \\
 &\quad \times \frac{1}{\mathcal{B}(\Lambda \rightarrow p \pi)^2 \mathcal{B}(D^0 \rightarrow X)}, \quad (5)
 \end{aligned}$$

where $N(\bar{B}^0 \rightarrow D^0 \Lambda \bar{\Lambda})$ is the fitted signal yield, $N_{B^0 \bar{B}^0}$ the number of the $B^0 \bar{B}^0$ pairs assuming $\mathcal{B}(\Upsilon(4S)4S \rightarrow B^0 \bar{B}^0) = 0.5$, $\bar{\epsilon}$ the average reconstruction efficiency, and $\mathcal{B}(\Lambda \rightarrow p \pi)$ and $\mathcal{B}(D^0 \rightarrow X)$ the branching fractions for the daughter decays of Λ and D^0 , respectively. An analogous expression holds for $\mathcal{B}(\bar{B}^0 \rightarrow D^0 \Sigma^0 \bar{\Lambda})$. The average efficiency $\bar{\epsilon}$ is defined as $N_{\text{rec}}/N_{\text{gen}}$ using signal MC events, where N_{rec} is the number of reconstructed signal events after all cuts and N_{gen} the number of all generated events assuming a phase space distribution.

We perform a simultaneous fit of the three D^0 decay channels to obtain

$$\begin{aligned}
 N_\Lambda &= \frac{N(\bar{B}^0 \rightarrow D^0 \Lambda \bar{\Lambda})}{\bar{\epsilon}^\Lambda \mathcal{B}(D^0 \rightarrow X)}, \\
 N_{\Sigma^0} &= \frac{N(\bar{B}^0 \rightarrow D^0 \Sigma^0 \bar{\Lambda})}{\bar{\epsilon}^{\Sigma^0} \mathcal{B}(D^0 \rightarrow X)}. \quad (6)
 \end{aligned}$$

The likelihood function is given by

$$\begin{aligned}
 L &= \prod_j \frac{e^{-(\bar{\epsilon}_j^\Lambda \mathcal{B}_j N_\Lambda + N_j^{\text{Bkg}} + \bar{\epsilon}_j^{\Sigma^0} \mathcal{B}_j N_{\Sigma^0})}}{N(j)!} \\
 &\quad \times \prod_k^{N(j)} [\bar{\epsilon}_j^\Lambda \mathcal{B}_j N_\Lambda f_j^\Lambda(m_{ESk}, m(D^0 \Lambda \bar{\Lambda})_k) \\
 &\quad + N_j^{\text{Bkg}} f_j^{\text{Bkg}}(m_{ESk}, m(D^0 \Lambda \bar{\Lambda})_k) \\
 &\quad + \bar{\epsilon}_j^{\Sigma^0} \mathcal{B}_j N_{\Sigma^0} f_j^{\Sigma^0}(m_{ESk}, m(D^0 \Lambda \bar{\Lambda})_k)], \quad (7)
 \end{aligned}$$

where \mathcal{B}_j is the branching fraction for the j th D^0 decay, N_j^{Bkg} the number of combinatorial background events in the j th subsample, N_Λ and N_{Σ^0} the yields of $\bar{B}^0 \rightarrow D^0 \Lambda \bar{\Lambda}$ and $\bar{B}^0 \rightarrow D^0 \Sigma^0 \bar{\Lambda}$, and $\bar{\epsilon}_j^\Lambda$ and $\bar{\epsilon}_j^{\Sigma^0}$ the average efficiencies for the j th D^0 decay.

V. SYSTEMATIC UNCERTAINTIES

We consider the following systematic uncertainties: the uncertainties associated with the number of $B\bar{B}$ events, the particle identification (PID) algorithm, the tracking algorithm, the π^0 reconstruction, the D^0 and Λ branching fractions, the efficiency correction, and the fitting algorithm.

The uncertainty associated with the number of $B\bar{B}$ pairs is 0.6%. We determine the systematic uncertainty associated with the PID by applying different PID selections and comparing the result with the nominal selection. The difference is 0.8%, which is assigned as the PID uncertainty. The systematic uncertainty associated with the tracking algorithm depends on the number of charged

tracks in the decay. We assign a systematic uncertainty of 0.9% for the $D^0 \rightarrow K^- \pi^+$ and $D^0 \rightarrow K^- \pi^+ \pi^0$ decays and 1.2% for the $D^0 \rightarrow K^- \pi^+ \pi^+ \pi^-$ decay. A 3% uncertainty is assigned to account for the π^0 reconstruction in $D^0 \rightarrow K^- \pi^+ \pi^0$ decays. A detailed description of these detector-related systematic uncertainties is given in Ref. [18].

We rely on the known D^0 branching fractions in our fit. To estimate the associated systematic uncertainty we vary each branching fraction by one standard deviation of its uncertainty [1] and define the systematic uncertainty to be the maximum deviation observed with respect to the nominal analysis. We divide $m(\Lambda\bar{\Lambda})$ into six bins and determine the total reconstruction efficiency ε_i in each bin. We determine the uncertainty due to the use of the average efficiency $\bar{\varepsilon}$ by studying $|\varepsilon_i - \bar{\varepsilon}|/\bar{\varepsilon}$ as a function of $m(\Lambda\bar{\Lambda})$. We average these values and take the result of 16.3% ($D^0 \rightarrow K^- \pi^+$), 19.6% ($D^0 \rightarrow K^- \pi^+ \pi^0$), and 16.8% ($D^0 \rightarrow K^- \pi^+ \pi^+ \pi^-$) as our estimate of the systematic uncertainty for the efficiency. We estimate the systematic uncertainty due to the fit procedure by independently varying the fit ranges of m_{ES} and $m(D^0 \Lambda\bar{\Lambda})$. The largest differences in the signal yield are 3.9% for the change of the m_{ES} fit range and 2.1% for the change of the $m(D^0 \Lambda\bar{\Lambda})$ fit range. To check our background model, we use a second-order polynomial in $m(D^0 \Lambda\bar{\Lambda})$ instead of a first-order polynomial. The signal yield changes by 1.1%. We use an ensemble of simulated data samples reflecting our fit results to verify the stability of the fit. We generate 1000 such samples with shapes and yields fixed to our results and repeat the final fit. We find no bias in the signal-yield results. All systematic uncertainties are summarized in Table II.

The total systematic uncertainty, obtained by adding all sources in quadrature, is 20.1%.

TABLE II. Summary of the systematic uncertainties for $\bar{B}^0 \rightarrow D^0 \Lambda\bar{\Lambda}$.

Source	Relative uncertainty
Additive uncertainty	
Fit procedure	4.6%
Multiplicative uncertainties	
$B\bar{B}$ counting	0.6%
Particle identification	0.8%
Tracking	
$D^0 \rightarrow K^- \pi^+$	0.9%
$D^0 \rightarrow K^- \pi^+ \pi^0$	0.9%
$D^0 \rightarrow K^- \pi^+ \pi^+ \pi^-$	1.2%
π^0 systematics	
$D^0 \rightarrow K^- \pi^+ \pi^0$	3.0%
D^0 and Λ branching fractions	2.9%
Variation over phase space	
$D^0 \rightarrow K^- \pi^+$	16.3%
$D^0 \rightarrow K^- \pi^+ \pi^0$	19.6%
$D^0 \rightarrow K^- \pi^+ \pi^+ \pi^-$	16.8%
Total uncertainty	20.1%

VI. RESULTS

The one-dimensional projections of the fit are shown in Fig. 4. We find

$$\begin{aligned} N_{\Lambda} &= 1880^{+560}_{-500}, \\ N_{\Sigma^0} &= 2870^{+1680}_{-1560}. \end{aligned} \quad (8)$$

The statistical significance is calculated as $\sqrt{-2 \log L_0/L_S}$, where L_0 is the likelihood value for a fit without a signal component and L_S is the likelihood value for the nominal fit. The statistical significance of the combined $\bar{B}^0 \rightarrow D^0 \Lambda\bar{\Lambda}$ and $\bar{B}^0 \rightarrow D^0 \Sigma^0 \bar{\Lambda}$ yields is 3.9 standard deviations (σ), while those of the individual $\bar{B}^0 \rightarrow D^0 \Lambda\bar{\Lambda}$ and $\bar{B}^0 \rightarrow D^0 \Sigma^0 \bar{\Lambda}$ results are 3.4σ and 1.2σ , respectively. Multiplicative systematic uncertainties do not affect the signal significance. Additive systematic uncertainties affecting the significance are negligible in this analysis compared to the statistical uncertainty. We therefore quote the statistical significance as the global significance.

The branching fractions are

$$\begin{aligned} \mathcal{B}(\bar{B}^0 \rightarrow D^0 \Lambda\bar{\Lambda}) &= (9.8^{+2.9}_{-2.6} \pm 1.9) \times 10^{-6}, \\ \mathcal{B}(\bar{B}^0 \rightarrow D^0 \Sigma^0 \bar{\Lambda} + \bar{B}^0 \rightarrow D^0 \Lambda\bar{\Sigma}^0) &= (15^{+9}_{-8} \pm 3) \times 10^{-6}, \end{aligned} \quad (9)$$

where the first uncertainties represent the statistical uncertainties and the second the systematic uncertainties. As a cross-check of the method, independent fits to the three subsamples are performed. The results of each of these fits are consistent with each other and with the nominal combined fit.

Since the statistical significance for $\mathcal{B}(\bar{B}^0 \rightarrow D^0 \Sigma^0 \bar{\Lambda} + \bar{B}^0 \rightarrow D^0 \Lambda\bar{\Sigma}^0)$ is low, a Bayesian upper limit at the 90% confidence level is calculated by integrating the likelihood function,

$$\mathcal{B}(\bar{B}^0 \rightarrow D^0 \Sigma^0 \bar{\Lambda} + \bar{B}^0 \rightarrow D^0 \Lambda\bar{\Sigma}^0) < 3.1 \times 10^{-5}. \quad (10)$$

To investigate the threshold dependence, we perform the fit in bins of $m(\Lambda\bar{\Lambda})$ and examine the resulting distribution after accounting for the reconstruction efficiency and D^0 branching fractions. The results are shown in Fig. 5. No significant enhancement in the $\bar{B}^0 \rightarrow D^0 \Lambda\bar{\Lambda}$ event rate is observed at the baryon-antibaryon mass threshold within the uncertainties, in contrast to $\bar{B}^0 \rightarrow D^0 p\bar{p}$ decays, which do exhibit such an enhancement [8].

We compare our results for the $\bar{B}^0 \rightarrow D^0 \Lambda\bar{\Lambda}$ and $\bar{B}^0 \rightarrow D^0 \Sigma^0 \bar{\Lambda}$ branching fractions to theoretical predictions. The result we obtain for the $\bar{B}^0 \rightarrow D^0 \Sigma^0 \bar{\Lambda}$ branching fraction is consistent with the prediction of $\mathcal{B}(\bar{B}^0 \rightarrow D^0 \Sigma^0 \bar{\Lambda} + \bar{B}^0 \rightarrow D^0 \Lambda\bar{\Sigma}^0) = (18 \pm 5) \times 10^{-6}$ from Ref. [11]. However, the obtained result for the $\bar{B}^0 \rightarrow D^0 \Lambda\bar{\Lambda}$ branching fraction is larger than the prediction of $\mathcal{B}(\bar{B}^0 \rightarrow D^0 \Lambda\bar{\Lambda}) = (2 \pm 1) \times 10^{-6}$ [11] by a factor of

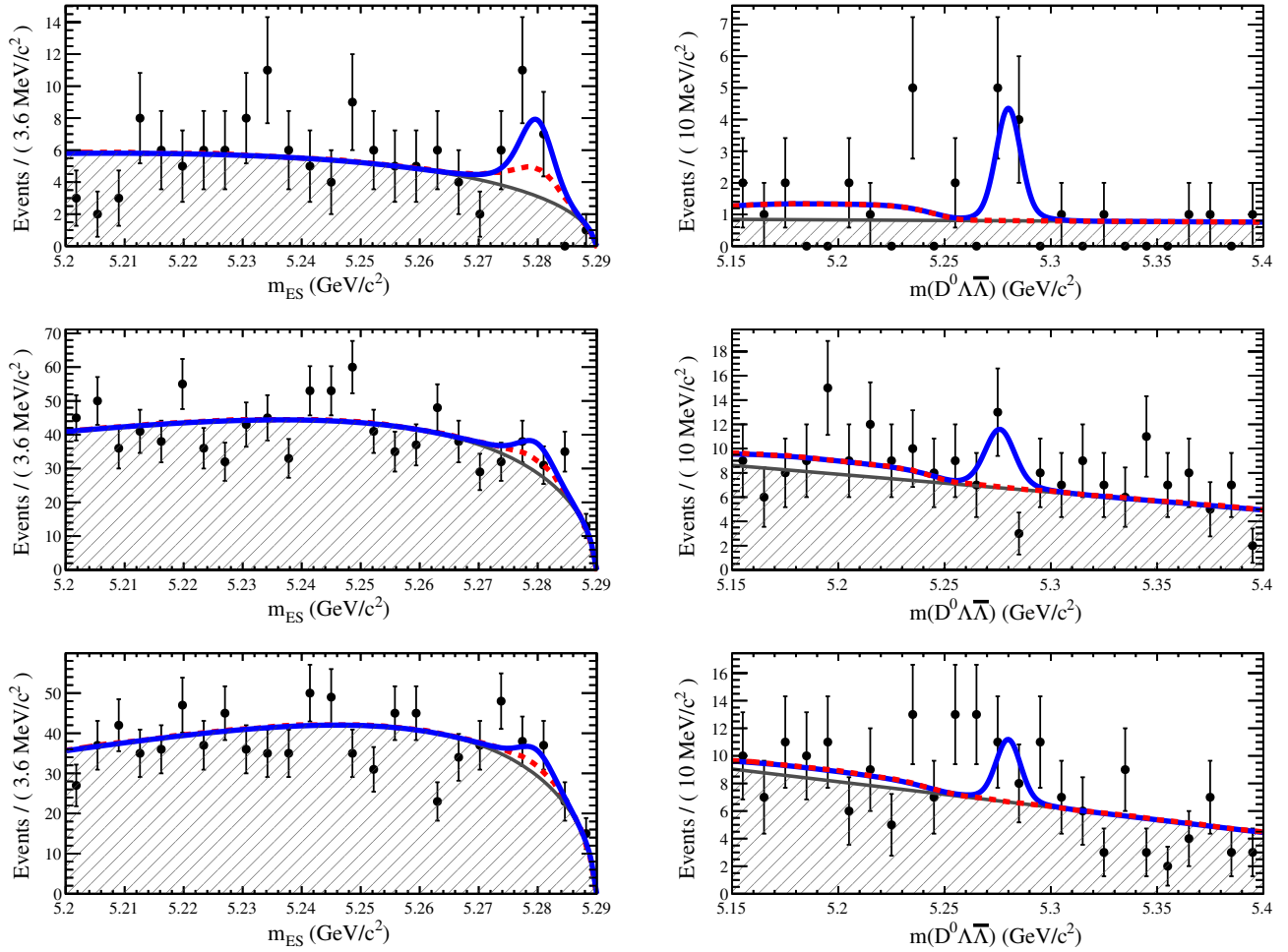


FIG. 4 (color online). Results of the combined fit. The m_{ES} projection is shown for $m(D^0 \Lambda \bar{\Lambda}) \in [5.15, 5.31]$ GeV/c^2 and the $m(D^0 \Lambda \bar{\Lambda})$ projection for $m_{ES} \in [5.272, 5.286]$ GeV/c^2 . The solid line shows the result of the fit, the dashed curve indicates the $\bar{B}^0 \rightarrow D^0 \Sigma^0 \bar{\Lambda}$ contribution, and the shaded histogram the combinatorial background. From top to bottom: $D^0 \rightarrow K^- \pi^+$, $D^0 \rightarrow K^- \pi^+ \pi^0$, and $D^0 \rightarrow K^- \pi^+ \pi^+ \pi^-$ subsamples.

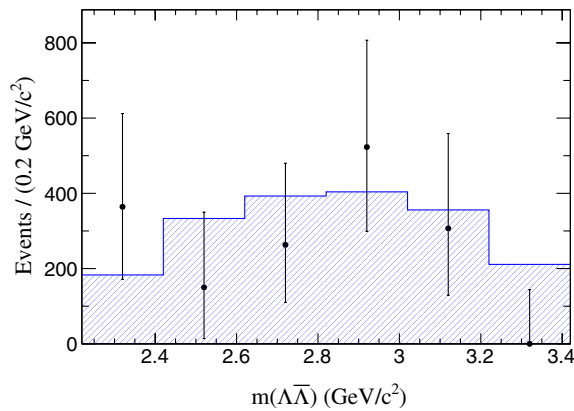


FIG. 5 (color online). Distribution of the invariant baryon-antibaryon mass for D^0 -branching-fraction and efficiency-corrected $\bar{B}^0 \rightarrow D^0 \Lambda \bar{\Lambda}$ signal candidates. The data points represent the *BABAR* data and the shaded histogram indicates phase-space-distributed simulated events, scaled to match the area under the data.

$$\frac{\mathcal{B}(\bar{B}^0 \rightarrow D^0 \Lambda \bar{\Lambda})_{\text{exp}}}{\mathcal{B}(\bar{B}^0 \rightarrow D^0 \Lambda \bar{\Lambda})_{\text{theo}}} = 4.9 \pm 3.0. \quad (11)$$

We further determine

$$\frac{\mathcal{B}(\bar{B}^0 \rightarrow D^0 \Sigma^0 \bar{\Lambda} + \bar{B}^0 \rightarrow D^0 \Lambda \bar{\Sigma}^0)}{\mathcal{B}(\bar{B}^0 \rightarrow D^0 \Lambda \bar{\Lambda})} = 1.5 \pm 0.9, \quad (12)$$

which is in agreement with our assumption that all four modes $\bar{B}^0 \rightarrow D^0 \Lambda \bar{\Lambda}$, $\bar{B}^0 \rightarrow D^0 \Sigma^0 \bar{\Lambda}$, $\bar{B}^0 \rightarrow D^0 \Lambda \bar{\Sigma}^0$, and $\bar{B}^0 \rightarrow D^0 \Sigma^0 \bar{\Sigma}^0$ are produced at equal rates. For the ratio of branching fractions, we find

$$\frac{\mathcal{B}(\bar{B}^0 \rightarrow D^0 \Lambda \bar{\Lambda})}{\mathcal{B}(\bar{B}^0 \rightarrow D^0 p \bar{p})} = \frac{1}{10.6 \pm 3.7}, \quad (13)$$

using $\mathcal{B}(\bar{B}^0 \rightarrow D^0 p \bar{p}) = (1.04 \pm 0.04) \times 10^{-4}$ [1]. This is in agreement with the expected suppression of 1/12 discussed in the Introduction.

VII. SUMMARY

We find evidence for the baryonic B decay $\bar{B}^0 \rightarrow D^0 \Lambda \bar{\Lambda}$. We determine the branching fraction to be $\mathcal{B}(\bar{B}^0 \rightarrow D^0 \Lambda \bar{\Lambda}) = (9.8_{-2.6}^{+2.9} \pm 1.9) \times 10^{-6}$ with a significance of 3.4σ including additive systematic uncertainties. This is in agreement with the Belle measurement [13]. Within the statistical uncertainty, our results support either a moderate threshold enhancement or no enhancement at all. The result for the branching fraction is in agreement within 1.3 standard deviations with theoretical predictions based on measurements of $\bar{B}^0 \rightarrow D^0 p \bar{p}$ and with simple models of hadronization. We find no evidence for the decay $\bar{B}^0 \rightarrow D^0 \Sigma^0 \bar{\Lambda}$ and calculate a Bayesian upper limit at 90% confidence level of $\mathcal{B}(\bar{B}^0 \rightarrow D^0 \Sigma^0 \bar{\Lambda} + \bar{B}^0 \rightarrow D^0 \Lambda \bar{\Sigma}^0) < 3.1 \times 10^{-5}$. This result is in agreement with the theoretical expectation.

ACKNOWLEDGMENTS

We are grateful for the extraordinary contributions of our PEP-II colleagues in achieving the excellent luminosity and machine conditions that have made this work possible.

The success of this project also relies critically on the expertise and dedication of the computing organizations that support BABAR. The collaborating institutions wish to thank SLAC for its support and the kind hospitality extended to them. This work is supported by the U.S. Department of Energy and National Science Foundation, the Natural Sciences and Engineering Research Council (Canada), the Commissariat à l’Energie Atomique and Institut National de Physique Nucléaire et de Physique des Particules (France), the Bundesministerium für Bildung und Forschung and Deutsche Forschungsgemeinschaft (Germany), the Istituto Nazionale di Fisica Nucleare (Italy), the Foundation for Fundamental Research on Matter (The Netherlands), the Research Council of Norway, the Ministry of Education and Science of the Russian Federation, Ministerio de Ciencia e Innovación (Spain), and the Science and Technology Facilities Council (United Kingdom). Individuals have received support from the Marie-Curie IEF program (European Union), the A. P. Sloan Foundation (USA) and the Binational Science Foundation (USA-Israel).

-
- [1] J. Beringer *et al.* (Particle Data Group), *Phys. Rev. D* **86**, 010001 (2012) and 2013 partial update for the 2014 edition.
 - [2] D. S. Carlstone, S. P. Rosen, and S. Pakvasa, *Phys. Lett.* **174**, 1877 (1968).
 - [3] N. Gabychev *et al.* (Belle Collaboration), *Phys. Rev. Lett.* **97**, 242001 (2006).
 - [4] B. Aubert *et al.* (BABAR Collaboration), *Phys. Rev. D* **78**, 112003 (2008).
 - [5] B. Aubert *et al.* (BABAR Collaboration), *Phys. Rev. D* **72**, 051101 (2005).
 - [6] J. T. Wei *et al.* (Belle Collaboration), *Phys. Lett. B* **659**, 80 (2008).
 - [7] R. Aaij *et al.* (LHCb Collaboration), *Phys. Rev. D* **88**, 052015 (2013).
 - [8] P. del Amo Sanchez *et al.* (BABAR Collaboration), *Phys. Rev. D* **85**, 092017 (2012).
 - [9] K. Abe *et al.* (Belle Collaboration), *Phys. Rev. Lett.* **89**, 151802 (2002).
 - [10] C. H. Chen, H.-Y. Cheng, C. Geng, and Y. Hsiao, *Phys. Rev. D* **78**, 054016 (2008).
 - [11] Y. K. Hsiao, *Int. J. Mod. Phys. A* **24**, 3638 (2009).
 - [12] G. Lafferty, *J. Phys. G* **23**, 731 (1997).
 - [13] Y. W. Chang *et al.* (Belle Collaboration), *Phys. Rev. D* **79**, 052006 (2009).
 - [14] J. P. Lees *et al.* (BABAR collaboration), *Nucl. Instrum. Methods Phys. Res., Sect. A* **726**, 203 (2013).
 - [15] D. J. Lange, *Nucl. Instrum. Methods Phys. Res., Sect. A* **462**, 152 (2001).
 - [16] S. Agostinelli *et al.* (GEANT4 Collaboration), *Nucl. Instrum. Methods Phys. Res., Sect. A* **506**, 250 (2003).
 - [17] B. Aubert *et al.* (BABAR Collaboration), *Nucl. Instrum. Methods Phys. Res., Sect. A* **479**, 1 (2002).
 - [18] B. Aubert *et al.* (BABAR Collaboration), *Nucl. Instrum. Methods Phys. Res., Sect. A* **729**, 2013 (615).
 - [19] Throughout this paper, all decay modes include the charge conjugated process.
 - [20] A. Drescher, B. Gräwe, B. Hahn, B. Ingelbach, U. Matthiesen, H. Scheck, J. Spengler, and D. Wegener, *Nucl. Instrum. Methods Phys. Res., Sect. A* **237**, 464 (1985).
 - [21] J. C. Anjos *et al.* (E691 Collaboration), *Phys. Rev. D* **48**, 56 (1993).
 - [22] G. C. Fox and S. Wolfram, *Phys. Rev. Lett.* **41**, 1581 (1978).
 - [23] H. Albrecht *et al.* (ARGUS Collaboration), *Phys. Lett. B* **241**, 278 (1990).